

Venous blood clot structure characterization using scattering operator

T. Berthomier^{1,2}, A. Mansour¹, L. Bressollette², F. Le Roy¹, D. Mottier²

¹LABSTICC, ENSTA Bretagne
2 rue François Verny, 29200 Brest, France
thibaud.berthomier@ensta-bretagne.org, mansour@ieee.org,
frederic.le_roy@ensta-bretagne.fr

²INSERM CIC 1412, CHRU de Brest
Boulevard Tanguy Prigent, 29200 Brest, France
luc.bressollette@chu-brest.fr,
dominique.mottier@chu-brest.fr

Abstract— Deep venous thrombosis (DVT) occurs when a blood clot appear within a deep vein, usually in the legs. The main complication is pulmonary embolism (PE) which is the third cause of vascular death after myocardial infarction and cardiovascular event. DVT onset is multifactorial (immobilization, surgery, age, cancers, genetic variations) and it is mostly diagnosed via ultrasound. In our project, we are interested in a new approach, which consists in using ultrasound and elastography to assess the mechanical properties of blood clots and to identify the thrombosis triggering factors. This means characterizing its structure, establishing his age, the cause of its formation and the risk of PE. In this paper, we aim to analyze the clot texture using the scattering operator which combines wavelet transform convolutions with non-linear modulus and averaging operators. The scattering operator is showing promising results in signal processing and especially in image classification. Therefore, we will apply this operator to our database and discuss the results of our simulation at the end of this manuscript.

Index Terms— Deep Venous Thrombosis (DVT); ultrasound imaging; elastography; scattering operator; wavelet, thrombus.

I. INTRODUCTION

The abnormal formation of a blood clot in a blood vessel is named thrombosis. Symptoms related to thrombosis depend on location, size and structure. Our project considers only Deep Venous Thrombosis (DVT) *i.e.* blood clots that block partially or totally deep veins of the legs (popliteal, femoral, and iliac). The main complication occurs when a clot fragment comes off and travels to the lung. This process is named pulmonary embolism (PE). Virchow's triad [1] describes three physiopathological mechanisms that contribute, isolated or combined, to the development of DVT: (a) stasis (e.g. immobilization), (b) endothelial injury (e.g. catheter) and (c) hypercoagulability (e.g. hormone, cancer, genetic variations). More precisions on blood clot formation and risk factors are provided in Section II.

The three main signs of DVT are calf or ankle swelling, leg warm to the touch and leg pain or tenderness. These signs are not specific to DVT and some

people suffering from DVT may have none of these symptoms. In Section III, different diagnose techniques used by doctors are presented (e.g. angiography, ultrasound). The detection of this pathology is relatively simple yet; it is a lot more difficult to identify the thrombosis origins, age and to estimate the risk of PE. In the literature, we can find studies linking thrombosis maturity to clot elasticity ([2], [3], and [4]), determining the impact of genetic variations on the onset of a DVT ([5] and [6]) or estimating treatment efficiency ([7] and [8]). The objective of our project is to analyze the blood clot structure with the help of ultrasound and elastometry techniques in order to estimate the age, the origins and the risk of PE. Ultimately, a major stake will be the detection of cancer in an early stage on a patient victim of DVT. Section IV describes the scattering operator [9] and its simulation results obtain on clot ultrasound images. This multiscale operator is based on wavelet filter banks and modulus rectifiers. The originality of this manuscript is to evaluate this technique on our database. Indeed, the literature [10] and our previous industrial project show that the scattering operator have really good performances on texture classification.

II. BLOOD CLOT FORMATION AND BREAKDOWN

A. Blood circulation

Blood flows one-way through a closed system formed by different veins and arteries [11]. Oxygenated blood flows from the heart to various organs through arteries which have thick walls. Veins have thinner and elastic walls and take over from arteries to pull up oxygen impoverished blood back to the heart thank to four: (a) the heartbeat which maintains a continuous flow, (b) the diaphragmatic or deep breathing, (c) the muscle pump system (calf muscular contraction) and (d) the venous pump of the foot which is the first step in venous return of blood when walking. Moreover, veins include a valve system to avoid blood reflux. Prolonged immobilization due to plaster cast, bed rest or long distance flights slows down blood circulation and encourages the growth of venous thrombosis.

B. Hemostasis and fibrinolysis

The physiological process keeping blood within veins and stopping the bleeding in case of vessel injuries is called hemostasis [12]. Hemostasis consists of three main phases: (a) vascular spasm, (b) primary and (c) secondary hemostasis. The first one corresponds to the reduction of damaged vessel diameter so that the bleeding progressively slows down. Next, platelets begin to adhere to the cut edges of the vessel and release chemicals to attract even more platelets. The platelet plug formation stops the external bleeding and this second phase is called primary hemostasis. The secondary hemostasis defines the following mechanism: small molecules, called clotting factors, begin to create the clot and form a collagen fiber called fibrin. When the vessel is being repaired, a process named fibrinolysis starts dissolving the clot and prevents it from growing and causing thrombosis. Hemostasis or fibrinolysis disorder is therefore one of the risk factors for venous thrombosis.

C. Thrombosis and symptoms

Thrombosis occurs when a blood clot is formed and bleeding stop process does not start or when the fibrinolysis step is deficient. It manifests as an inflammation of a stamped or obstructed vessel due to the clot [11]. Venous thrombosis mostly appears in the legs. There are two levels of thrombosis: superficial and deep thrombosis. The first one comes out in the superficial veins *i.e.* in the veins near the skin and usually causes no fever, no infection and no swelling. It is dangerous because it can hide a deeper thrombosis or evolve to reach the deep venous network.

Deep Venous Thrombosis (DVT) is extremely dangerous because a piece or the entire deep vein clot could break off, be carried by the blood to the lung and cause a pulmonary embolism (PE). The clot formation often begins in the calf veins, where the blood flow may slow down (valves, collateral veins) and extends to the knee or thigh veins [12]. The risk of PE is that the clot gets closer to the heart. When a deep vein is obstructed by a clot, the blood cannot flow back to the heart through this vein; this creates a hypertension upstream part of the clot, so the blood has no other choice than to flow through the superficial venous network.

DVT can be revealed by three main signs: swelling of the calf or the ankle, leg warm to the touch and leg pain or tenderness. The symptoms of a DVT depend on the inflammatory response extend around the clot and on its size. The patient could also have numbing, cramps, a sensation of heavy legs, pain on palpation and/or bluish skin discoloration. At a confirmed stage, DVT may go along with fever, edema, ulcer, tachycardia or even a complete functional impotence [12]. Sometimes there is no symptom, making this disease even more dangerous. Moreover, relapse is frequent and the patient can have post-thrombotic symptoms *i.e.* long-term complications.

D. Risk factors

In normal conditions, there is a balance in the blood circulation among molecules of the coagulant and anticoagulant systems. Many physiopathological

mechanisms can unbalance the blood circulation and create a venous thrombosis. Virchow [1] has given a substantial contribution to our knowledge about the venous thromboembolism. Virchow's triad describes three mechanisms that contribute, isolated or combined, to the development of DVT: (a) stasis, (b) endothelial injury and (c) hypercoagulability

The first term of the Virchow's triad is stasis and gathers all factors responsible for the blood slow down. Extended immobilization due to a disease, a bed rest or a labor, plaster cast, heart failure, varicose vein and venous constriction because of a prolonged sitting, a long distance flight or a cancer contribute to reduce the blood flow and stimulate the appearance of thrombosis. For instance, statistics on venous thrombosis showed an incidence of two to four per ten thousand passengers of a flight over five hours [13]. Smoking also increases the risk as it stimulates the production of fibrinogen in the blood (and hence platelet aggregation and coagulation) and makes the blood more viscous. As a reaction, the number of red and white blood cells goes up in order to make up for oxygen insufficiency.

The second group of factors includes surgery, catheter, traumatism and age. These factors degrade venous walls; therefore an infection can cause an inflammation, so the return of blood in the vein can produce a thrombosis. Risks of DVT are stronger after a hospital discharge and with elderly patients. Statistics [13] show that the risks, without preventive thrombosis in medicine, increase in the range of ten to twenty percent in the four to five weeks following a hospital discharge. In the same way, risks become twice larger every ten years after the age of 40.

Hypercoagulability constitutes the third part of the triad and incorporates all mechanisms reinforcing coagulation or disturbing anticoagulation. It can be acquired factors (such as pregnancy, hormone therapy, and cancer), inflammatory disorders or inherited factors (Factor V Leiden mutation, protein C or S deficiency, antithrombin deficiency). Pregnant women or people with hormonal treatment have two to five times more likely to develop a DVT [13].

E. Diagnosis and treatment

In order to reduce the risk of PE, it is vital to diagnose as soon as possible the DVT. However, this task seems to be difficult because the signs and symptoms associated with the DTV are not specific to this disease [12]. D-dimer is a fibrin degradation that occurs in the blood after a clot is degraded by fibrinolysis. While the measure of D-dimer concentration allows excluding thromboembolic disease where the probability is low, a positive result does not always indicate thrombosis. Test using ultrasound dispel doubt of DVP: Doctors can view the blood network, see the blood flow and check on the veins' compressibility. A vein with a blood clot is relatively incompressible and is more echogenic than a free vein.

III. DIAGNOSTICAL TECHNIQUES

A. Common techniques

The difficulties in the diagnosis of the DVT are related to its characteristics often asymptomatic and the lack of specific clinical signs. The following items give the most commonly used methods to detect a DVP and to analyze the blood clot:

- By injected a contrast medium, venography (or phlebography or venous angiography) uses X-rays to examine the veins. Nowadays, this procedure is rarely applied because of its cost and its invasiveness. However, it still remains the gold standard for diagnosing DVT with imaging means.

- Using Magnetic Resonance Imaging (MRI), Magnetic Resonance Angiography (MRA) visualizes the blood vessels and examines the abnormalities of the arteries and less commonly of the veins. This method mostly involves intravenous contrast agents.

- Computed Tomography Angiography (CTA) is also an invasive technique but displays the anatomical detail of blood vessels more precisely than MRA or ultrasound. Its main application is screening for arterial disease because it is safer and less time-consuming than angiography.

- The main imaging technique to explore the deep venous network is Doppler ultrasonography. Ultrasonography allows to view the veins and to test the presence of a clot (compressibility and echogenic mark). The Doppler extension puts the blood flow up (or the absence of flow if the vein is blocked). The frequency of the used sound waves varies between 50 Hz and 20 kHz depending on the expected exploring depth [14].

B. A new approach : elastography/metry

In the medical context, the main application is the diagnosis of hepatic fibrosis because the liver gets harder when the fibrosis gets more severe. In old days, palpation was used to estimate the hardness. Recently, several systems can precisely measure and create a map of the organ hardness (elastography).

1) Principle

Elastometry consists in estimating the hardness, or the elasticity, of human tissues, e.g. their resistance when a mechanical force is applied on it: the harder a tissue is, the more elastic it is. A static external stress σ (in pascal Pa), applied to the surface of a solid, is linearly proportional to its fractional extension ε (non-dimensional) by the modulus of elasticity E (in Pa). This principle is named Hooke's law [2]:

$$\sigma = \varepsilon E \quad (1)$$

Human soft tissues can distort under the influence of two types of mechanical waves: compressional and shear waves. The first type is also called longitudinal waves because the particle displacement is parallel to the direction of wave propagation. The second type is equivalently called transverse waves because the particle displacement is perpendicular to the direction of the wave propagation. The velocity of these waves is directly

connected to the elastic modulus E (or Young's modulus). In soft biological tissues [15], the compressional velocity is far higher (≈ 1500 m/s) than the shear wave velocity (≈ 10 m/s), so the Young's modulus can be approximated using the following equation:

$$E \approx 3\rho c_s^2 \quad (2)$$

where ρ is the volume density (kg/m^3) and c_s the shear wave velocity (m/s). The volume density is assumed to be constant (1000 kg/m^3 which is the water density) even if it is actually different from one tissue to another (fat $\approx 950 \text{ kg/m}^3$, blood $\approx 1025 \text{ kg/m}^3$, liver $\approx 1060 \text{ kg/m}^3$, muscle $\approx 1070 \text{ kg/m}^3$ and bone between 1380 kg/m^3 and 1810 kg/m^3 [16]).

2) Current systems

Elastometry systems do not measure directly the hardness of the human tissue but estimate the velocity of the shear waves. These systems send either a mechanical or an acoustic impulse to generate the shear waves and follow their propagation using ultrasound, *i.e.* compressional waves. Ultrasonic echoes are analyzed in order to determine the velocity of the shear waves, and hence the elasticity. Currently, there are several systems able to quantify the hardness of biological tissues [17]:

- Fibroscan (Echosens): this system sends a mechanical impulse to create the shear waves and is mainly used to diagnose fibrosis and especially hepatic fibrosis. This method is quantitative.

- Virtual Touch Imaging (Siemens): the impulse is, here, ultrasonic. Ultrasound imaging allows the user to define the region of interest (ROI) on the target and the system computes the velocity of the shear waves in the ROI.

- Aixplorer (Supersonic Imagine): it operates similarly to the Virtual Touch Imaging system (ultrasonic shear waves and ROI) but the user can also display an elasticity map in a predefined window and get the mean elasticity in a ROI within this window. This technics is therefore both quantitative and qualitative.

- Aplio 500 (Toshiba): this system is close to the Aixplorer system and is used to create our database.

- Shear wave elastography mode is also proposed by other manufacturer such as Epiq (Philips), Arietta (Hitachi Aloka), Logic (General Electric), SonixTouch (Ultrasonix) and MyLabEight (Esaote).

IV. SCATTERING OPERATOR

A. Introduction

By applying the scattering operator, we would like to analyze the clot structure using ultrasound images. The database combines ultrasound images from 20 patients suffering from thrombosis. We choose to apply the scattering operator [9] on our database because this algorithm has given very good results on our previous industrial project which classifies acoustic images of the seabed.

The challenge of automatically classify signals and especially images resides in the high variability within a

same class of signals. This variability is often uninformative in the sense that it does not characterize a class change. The scattering operator aims at reducing this variability by creating a “translation invariant image representation, which is stable to deformations and preserves high frequency information for classification” [9].

B. Scattering wavelet

The translation invariance is obtained using a low-pass filter:

$$\phi_j(u) = 2^{-2j} \phi(2^{-j}u) \quad (3)$$

where 2^j is the maximum scale and u stands for the spatial position vector and ϕ is a scaling function named father wavelet. The first coefficient of the scattering transform of an image x is defined by the following equation:

$$S[\emptyset]x = x * \phi_j \quad (4)$$

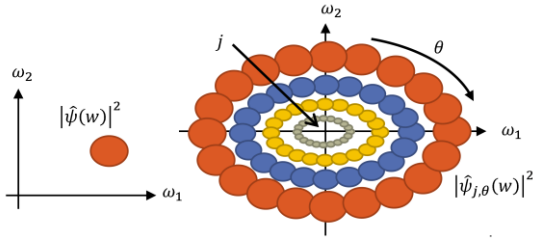


Figure 1: Frequency support of the mother wavelet on the left side and of the child wavelets on the right side: $\hat{\Psi}_\lambda$ is the Fourier transform of ψ_λ

The high-frequency information affected by this filter is recovered via two-dimensional wavelets. These wavelets are obtained by scaling and rotating a band-pass filter ψ (see Fig. 1). The number of rotations and scales are key parameters of the scattering transform. During the simulation, they are respectively fixed at four rotations and three scales (based on the literature). These located wavelets are defined, for each scale $0 < j < J$ and an orientation θ , by the following equation:

$$\psi_\lambda(u) = 2^{-2j} \psi(2^{-j} r_\theta^{-1} u) \quad (5)$$

where, to simplify notation, $\lambda = 2^{-j} r_\theta$

and r_θ is the rotation matrix: $r_\theta = \begin{bmatrix} \cos(\theta) & -\sin(\theta) \\ \sin(\theta) & \cos(\theta) \end{bmatrix}$.

The wavelet transform is stable to small deformation and invertible if the rotated and scaled wavelet filters cover the whole frequency plane. In the simulation, the Morlet wavelet family is used. The use of the norm $L_1(\mathbb{R}^2)$ on the wavelet coefficient modulus makes the representation translation -invariant:

$$\|x * \psi_\lambda\|_1 = \int_{\mathbb{R}^2} |x * \psi_\lambda(u)| du \quad (6)$$

The first layer of the scattering transform is thus defined by applying the average filter ϕ_j :

$$S[\lambda_1]x = |x * \psi_{\lambda_1}| * \phi_j \quad (7)$$

The integration, which removes all non-zero frequency components, causes an information loss. However, this information can be recovered by calculating the wavelet coefficients of $|x * \psi_{\lambda_1}|$. Therefore their $L_1(\mathbb{R}^2)$ norms define a larger family of invariants (second layer):

$$S[\lambda_1, \lambda_2]x = \left| |x * \psi_{\lambda_1}| * \psi_{\lambda_2} \right| * \phi_j \quad (8)$$

Further iteration on the wavelet transforms and the modulus operators enables evaluating more translation invariant coefficients:

$$S[p]x = \left| \left| |x * \psi_{\lambda_1}(u)| * \psi_{\lambda_2}(u) \right| \dots * \psi_{\lambda_m}(u) \right| * \phi_j(u) \quad (9)$$

where $p = (\lambda_1, \lambda_2, \dots, \lambda_m)$ is the set of all paths and m the number of layers.

C. Scattering representation

1) Application on a test image

In practice, only the first and the second layers are computed. These coefficients can be displayed as piecewise constant functions equal to $S[p]x$ over each frequency subset. Fig. 2 represents the scattering transform of an image with a striped pattern. The maximum coefficient corresponds to the orientation and the frequency (or scale) of the stripes: here the maximums correspond on the orientation 45° and the smallest scale.

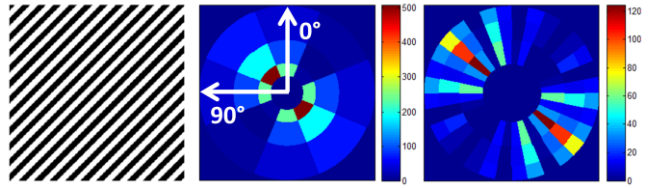


Figure 2: Scattering representation of stripes in the frequency plane: on the first layer (middle), each rotated quadrant has an area proportional to 2^{2j} ; on the second layer (right) each quadrant of the first is subdivided into a partition of subsets proportional to 2^{2j} .

2) Application on venous ultrasound images

Firstly, the scattering operator is applied on the entire image without specific preprocessing. The first row of Fig. 3 presents three ultrasound images, two of which come from the same patient but from two different legs. The first two images show the echography of, respectively, a free vein and a thrombosed vein. The inside of the vein is encircled by an ellipse drawn by a medical expert. The second and the third row of Fig. 3 show the associated scattering coefficients displayed in the frequency plane at the first and second order.

The size of the blood clot and the contrast between the vessels and the rest of the image differ among patients. The scattering coefficient of the entire image (vein, artery and tissue) should be different for two images taking from two different patients. Nevertheless, the results illustrated on Fig. 3 are difficult to be interpreted because the scattering coefficients seem very similar, especially at the first layer. On the second layer, we can see that the coefficient from patient 1 and 2 are quite different.

In the absence of thrombosis, the inside of the vein is darker than when there is a clot. The results are as well not really conclusive. The first order coefficients from the image without clot are very similar from those with clot. The second order coefficients are a little more different. Here, the images do not only content the inside of the vein (blood or clot) but also the artery and human tissue. Henceforth, the scattering operator does not allow us to characterize the blood clot. The next section will consider only images extracted within the ellipse.

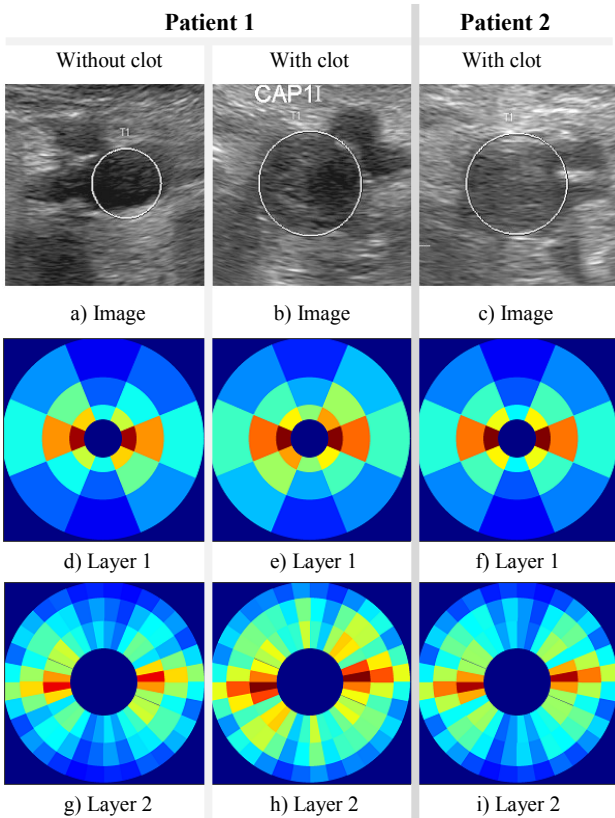


Figure 3: Three ultrasound images taken from two different patients (the inside of the vein is encircled); the first and the second layers of the scattering coefficients are represented in the frequency plane.

3) Application on blood clot ultrasound images

In this section, the scattering operator is applied only on blood clot images. To do so, we extracted the largest square image contained in the ellipse drawn by a medical expert. These small images are then resized using the discrete cosine transform and zero padding. After these two operations, we apply to them the scattering operator.

On Fig. 4, we can see these images and there scattering coefficients. The results seem more informative. On the first and the second layer, the coefficients with the maximum energy (red to yellow) are stronger for the two images with a clot. The second layer seems also making possible the discrimination between the two patients.

These positives results still require more investigation. Indeed, these results were obtained with one set of parameters, few images and without preprocessing.

V. SIMULATION

A. Experimental procedure

Our database contains 446 acquisitions obtained on 20 patients. The ultrasound images were generated with the same system (Aplio 500, Toshiba) but under different conditions (medical expert, echography mode, frequency and gain). In this article, we only consider the data collected with the most frequently used preset (about 200 images acquired with the same echography mode, frequency and gain). Indeed, the use of different presets

can affect the scattering coefficients and biased our conclusions. Our final goals are to identify the main causes of the DVT and to evaluate the risk of a PE. Thus we classify our data according to the patient physiopathology and the presence of PE:

- Cancer (canc.)
- Idiopathic (idio.)
- Idiopathic and PE (idio. PE)
- Immobilization (immo.)
- Pregnancy (preg.)
- Surgery and PE (surg. PE)

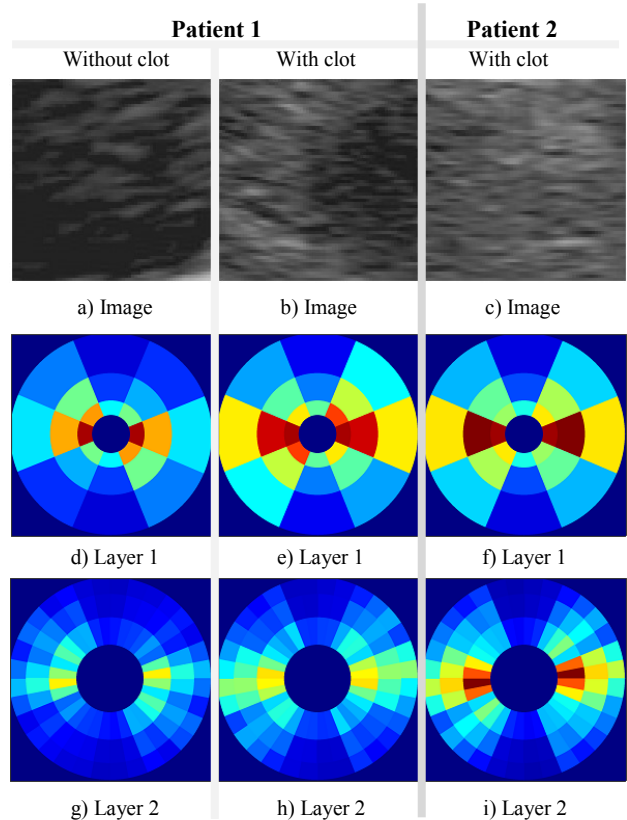


Figure 4: Same type of representation than Figure 3 except there is a zoom on the blood clot.

The scattering operator parameters (number of scales, orientations, orders and the size of the images) should be optimized. The optimization step is necessary; even though, there is no guarantee that it will lead to a satisfactory classification. We are not totally sure that the cause of the thrombosis and the presence of a PE are linked to the clot structure. In our simulation, we resize our images at 64 x 64 pixels because a power-of-2 square image simplifies the scattering calculation and because the average size of the extracted images is about 60x60 pixels. All coefficients are computed with the following parameters:

- Number of scales J : 2, 3, 4, 5, 6 and 7
- Number of orientations L : 1, 2, 4, 6 and 8.

The authors of [9] show that the scattering energy has an exponential decay with respect to the order m . In addition, this scattering energy converges to 0 as m

increases and is below 1% when $m \geq 3$. Therefore, all obtained coefficients (for all J and L) are neglected when $m \geq 3$. In this case, each image is represented by one vector per order (*i.e.* three vectors: orders $m = 0$, $m = 1$ and $m = 2$). After that, an Euclidean distance is used as discriminant information. Finally, we take into account the shear wave velocity through the blood clot. Indeed, for each acquisition, the system measures the velocity mean inside the region of interest (ROI).

B. First results

1) Scattering coefficients

Figure 5 represents the Euclidean distance among the scattering coefficients for each pair of images. We choose the first image as a reference image. During the experimentation, we change our reference without affecting much the outcomes. The three axes shown in Figure 5 correspond to coefficients computed at three different orders ($m = 0$, $m = 1$ and $m = 2$). Based on the obtained shapes, we can conclude that order 0 coefficients are more informative than those of order 1 and 2. Figure 7 considers only the order 0 and we can actually see that some patients stand apart from the others. The set of patients can be split into the two following groups;

- Group 1: No. 2, No. 4, No. 8 and No. 19;
- Group 2: No. 1, No. 9, No. 10, No. 13, No. 15, No. 16, No. 17 and No. 18.

However, it is difficult to link this observation with the main cause of the DVT. There is a pregnant woman in each group (No. 17 and No. 19). Idiopathic thromboses are also presented in the two groups.

The coefficients of patient 2 show the impact of the acquisition conditions. Indeed, two levels can be easily distinguished. In fact, these images were taken by two different medical experts. We can notice as well that there are two levels for patient 19: the beginning of the DVT and three months later. The age of the blood clot seems to impact the scattering coefficients. Naturally, an old blood clot is stiffer, and thus more echogenic than a recent blood clot. We are aiming to enrich our database, to compare the scattering coefficients according to the age of the thrombus.

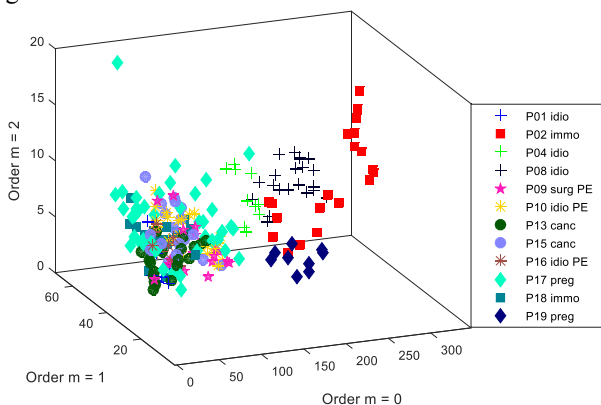


Figure 5: Euclidean distance among scattering coefficients of each image and the reference. Each axis represents the coefficient concatenation of each order. The marker indicates the patient number and its class (main triggering factor and presence of PE)

Moreover, the order 0 corresponds to low frequency information which depends greatly on the overall energy of the image. In order to characterize the clot structure, the higher scattering orders appear more appropriate. Nevertheless, looking at Figure 8 and Figure 9, the scattering coefficients seem to give less information and they change a lot for images of a same patient as the order m increases. The distance between patient 19 and the reference is, for example, much smaller at this order. Next paragraph considers the elastometry measures as discriminant information.

2) Shear waves velocity

In Figure 6, each image is described with three features: the velocity average of the shear waves through the clot, the 0-order and 1-order coefficients. As before, patient 2 stands apart in terms of the scattering coefficients. As well, the shear waves are faster in the clot of patient 13. Figure 10 confirms this observation but shows also that the velocity may vary significantly for a given patient (about 1 m/s for a value ranged from 1 to 5 m/s). Considering the patient 17, the shear waves seem strangely slower through the old clot than through the recent clot. The explanation could be the anticoagulant treatment which made it softer. To confirm this hypothesis, more data are required.

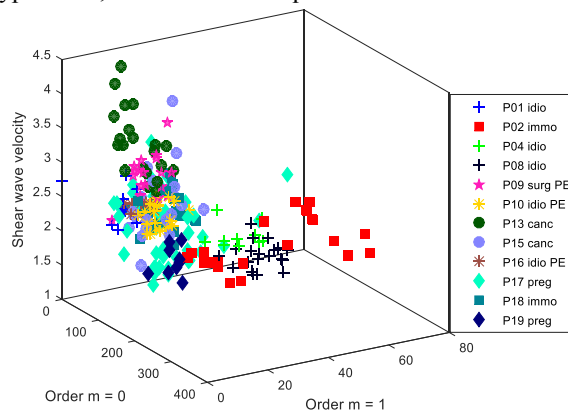


Figure 6: Combination of scattering coefficient (orders 0 and 1) and shear wave velocity (m/s). The marker indicates the patient number and its class (main triggered factor and presence of PE)

3) Partial conclusions

These experiments did not reveal much about a correlation among the blood clot structure, the scattering coefficients and the shear wave velocities. In our experimentation, we tried other metrics (*e.g.* Minkowski at different exponents), increased the size of the images (128x128 pixels) and considered the third order coefficients. But, unfortunately, these new parameters do not affect the results. Then, we attempt to reduce the number of coefficients using the discrete cosine transform [9] or the principal component analysis [10]. The goal is to keep only the most informative coefficients. After this reduction, Euclidean distances reduced features is evaluated. However, similar results were observed. This means that our reduction works but there is not enough information in the scattering coefficients to characterize the blood clot structure.

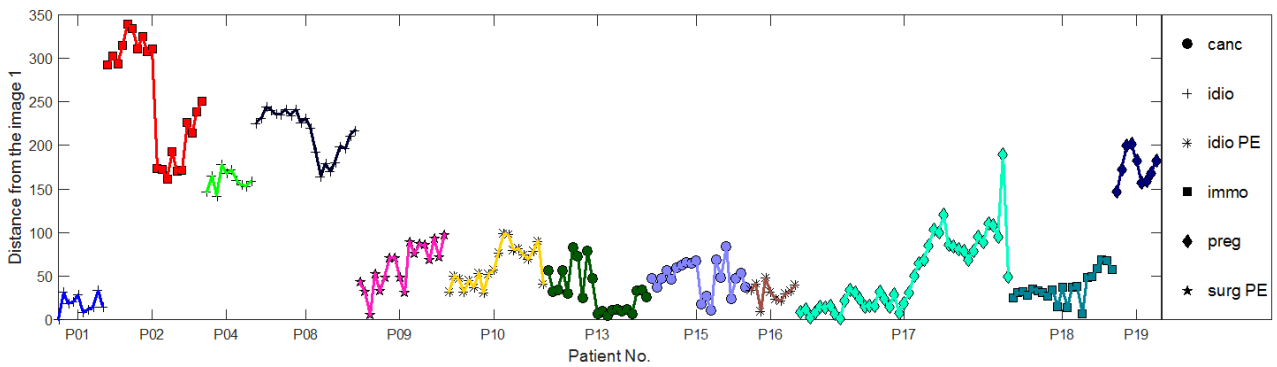


Figure 7: Euclidean distance between order 0 scattering coefficients of each image our reference (image 1). The x-axis corresponds to the patient number and the form of the markers indicates the physiopathology and the presence of a PE.

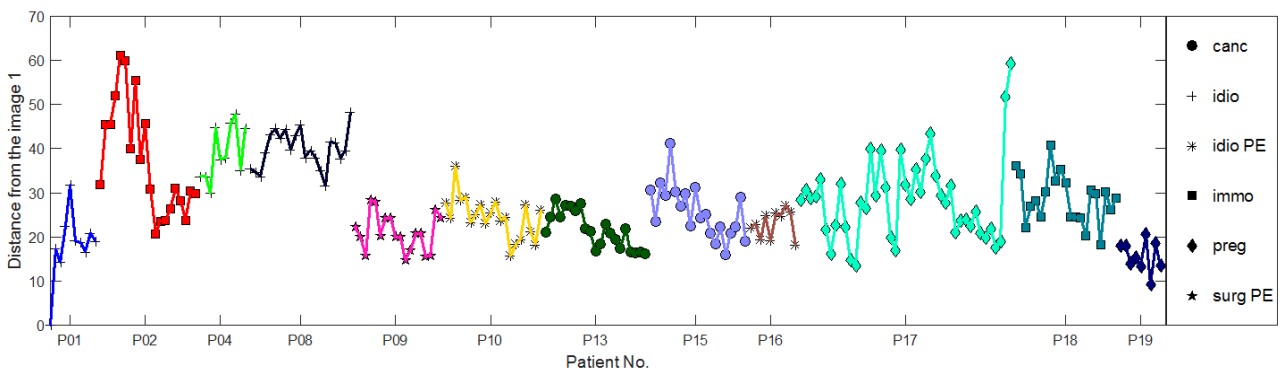


Figure 8: Euclidean distance between order 1 scattering coefficients of each image and our reference (image 1).

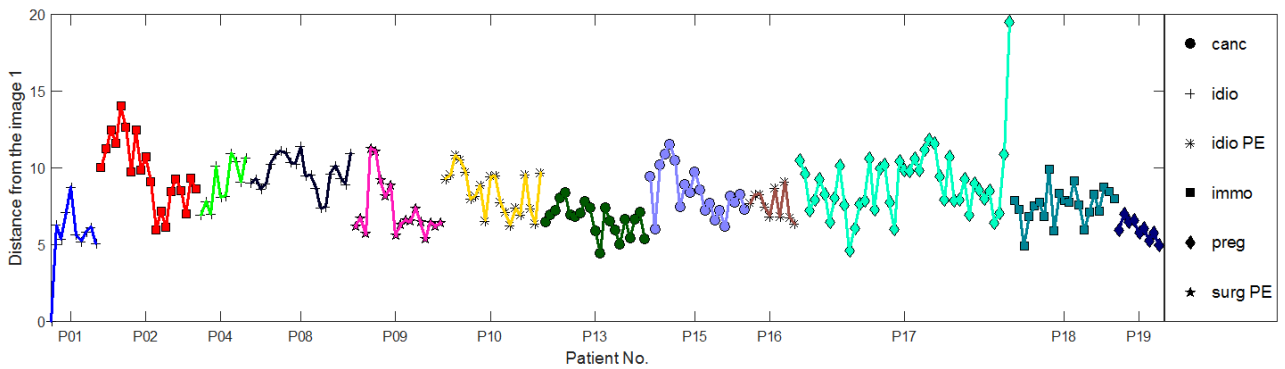


Figure 9: Euclidean distance between order 2 scattering coefficients of each image and our reference (image 1).

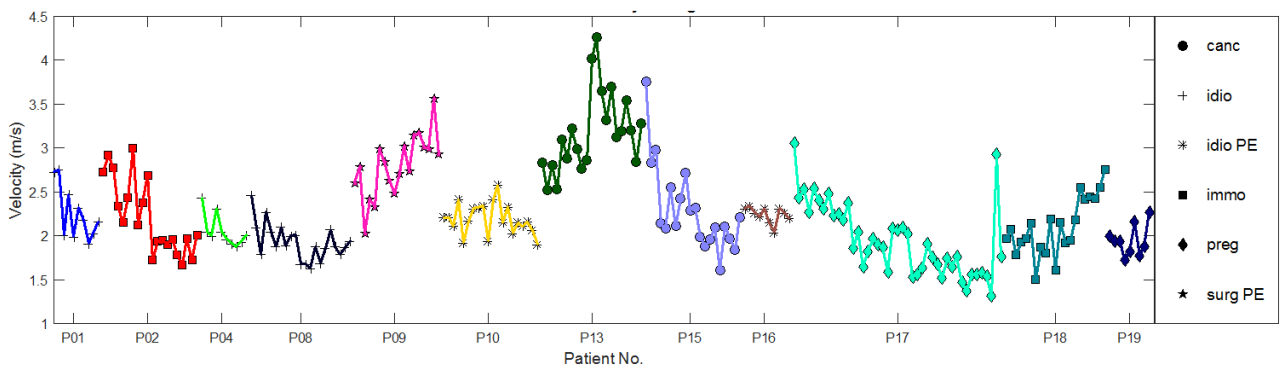


Figure 10: Shear wave mean velocity through the blood clot for each acquisition.

VI. CONCLUSION AND FUTURE WORK

Multiple factors can cause a deep venous thrombosis: stasis, endothelial injury or/and hypercoagulability. This disease is especially dangerous because it may be asymptotic and create a pulmonary embolism. In our project, we aim at characterizing the blood clot structure in order to date it, explain its formation and estimate the risk of PE. In this paper, we create a database of ultrasound clot images and apply the scattering operator. This algorithm, based on wavelet transforms, shows promising results for image classification. Nevertheless our simulation shows that the scattering operator seems to be not suited for clot characterization purposes. In future work, we will try to improve our results by using preprocessing techniques (e.g. histogram equalization), by making the scattering operator invariant to rotation and scale [18]. If the scattering results are not satisfactory, we are planning to explore statistical methods. Moreover, during our simulation, we used the elastometry data (shear wave velocity through the clot) without the elastography (shear wave velocity map of the clot). Recently, we get a new probe and our acquisition system is updated so we will be able to build a larger and higher quality database.

REFERENCES

- [1] C. N. Bagot and R. Arya, "Virchow and his triad: a question of attribution," *British Journal of Haematology*, vol. 143, no. 2, pp. 180–190, Oct. 2008.
- [2] S. Beuil, "Recherche d'une corrélation entre l'échographie 2D et l'Elastométrie sur les thromboses veineuses proximales profondes pour datation du thrombus," Mémoire de DESC de médecine vasculaire, UBO, Brest, 2013.
- [3] B. Geier, L. Barbera, D. Muth-Werthmann, S. Siebers, H. Ermert, S. Philippou, and A. Mumme, "Ultrasound elastography for the age determination of venous thrombi. Evaluation in an animal model of venous thrombosis," *Journal of Thrombosis and Haemostasis*, Jan. 2005.
- [4] J.-L. Gennisson, S. Lerouge, and G. Cloutier, "Assessment by transient elastography of the viscoelastic properties of blood during clotting," *Ultrasound in Medicine & Biology*, vol. 32, no. 10, pp. 1529–1537, Oct. 2006.
- [5] Smith NL, Hindorff LA, Heckbert SR, Lemaitre RN, Marcianti KD, Rice K, Lumley T, Bis JC, Wiggins KL, Rosendaal FR, and Psaty BM, "Association of genetic variations with nonfatal venous thrombosis in postmenopausal women," *Journal of the American Medical Association*, vol. 297, no. 5, pp. 489–498, Feb. 2007.
- [6] F. Couturaud, C. Leroyer, C. Tromeur, J. A. Julian, S. R. Kahn, J. S. Ginsberg, P. S. Wells, J. D. Douketis, D. Mottier, and C. Kearon, "Factors that predict thrombosis in relatives of patients with venous thromboembolism," *Blood Journal*, vol. 124, no. 13, pp. 2124–2130, Sep. 2014.
- [7] F. Couturaud, O. Sanchez, G. Pernod, P. Mismetti, P. Jégou, E. Duhamel, K. Provost, C. B. dit Sollier, E. Presles, and P. Castellant, "Six Months vs Extended Oral Anticoagulation After a First Episode of Pulmonary Embolism: The PADIS-PE Randomized Clinical Trial," *The Journal of the American Medical Association*, vol. 314, no. 1, pp. 31–40, 2015.
- [8] H. R. Büller, H. Décousus, M. A. Grosso, M. Mercuri, S. Middeldorp, M. H. Prins, G. E. Raskob, S. M. Schellong, L. Schwöcho, A. Segers, M. Shi, P. Verhamme, and P. Wells, "Edoxaban versus warfarin for the treatment of symptomatic venous thromboembolism," *The New England Journal of Medicine*, vol. 369, no. 15, pp. 1406–1415, Oct. 2013.
- [9] J. Bruna and S. Mallat, "Invariant Scattering Convolution Networks," *IEEE Transactions on Pattern Analysis and Machine Intelligence*, vol. 35, no. 8, pp. 1872–1886, Aug. 2013.
- [10] J. Bruna and S. Mallat, "Classification with scattering operators," *Computer Vision and Pattern Recognition*, pp. 1561–1566, 2011.
- [11] A. M. N. Gardner and R. H. Fox, *The Venous System in Health and Disease*. IOS Press, 2001.
- [12] R. W. Colman, *Hemostasis and Thrombosis: Basic Principles and Clinical Practice*. Lippincott Williams & Wilkins, 2006.
- [13] P. Léger, D. Barcat, C. Boccalon, J. Guilloux, and H. Boccalon, "Thromboses veineuses des membres inférieurs et de la veine cave inférieure," *EMC - Cardiologie-Angéiologie*, vol. 1, no. 1, pp. 80–96, Feb. 2004.
- [14] N. Grenier and M. Claudon, "Bases physiques du Doppler," in *Echo-doppler*, Société Française de la Radiologie., vol. 1, 1 vols., Paris, 1995, p. 13.
- [15] M. E. Hachemi, S. Callé, and J.-P. Remeniéras, "Application of shear wave propagation to elasticity imaging of biological tissues," *Traitement du signal et cancérologie*, vol. 23, 2006.
- [16] L. M. Roch, "Introduction à l'imagerie médicale," University of Montreal Hospital, Mar-2006.
- [17] M. Wagner, C. Pellot-Barrakat, S. Rasian, I. Huynh, S. Egels, F. Frouin, and O. Lucidarme, "L'élastographie ultrasonore: il est temps de faire un état des lieux," presented at the Journée Francophones de Radiologie 2013, Paris, 2013.
- [18] L. Sifre and S. Mallat, "Rotation, scaling and deformation invariant scattering for texture discrimination," in *Proceedings of the IEEE Conference on Computer Vision and Pattern Recognition*, 2013, pp. 1233–1240.